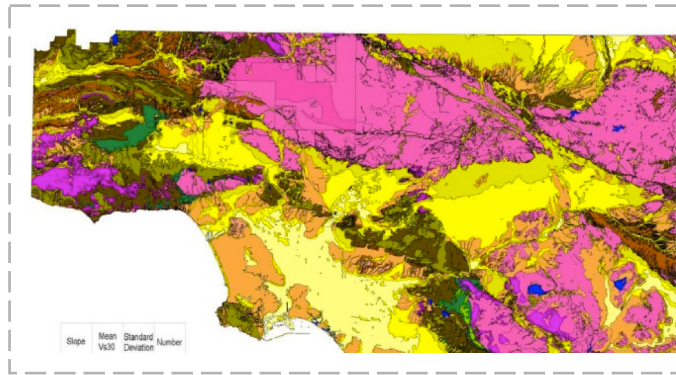


Define a Consistent Strategy to Model Ground Motion: Site Effects in Parametric Ground Motions

Report produced in the context of the Global Project
“GEM Ground Motion Prediction Equations”



Jonathan P. Stewart¹, David M. Boore², Ken Campbell³, Mustafa Erdik⁴,
Walter Silva⁵

¹ University of California, Los Angeles, ² U.S. Geological Survey, ³ EQECAT, ⁴ Bogazici University, ⁵ Pacific Engineering and Analysis



Define a Consistent Strategy to Model Ground Motion: Site Effects in Parametric Ground Motion Models

GEM Ground Motion Prediction Equations

Version: 1.0.0

Author(s): Jonathan P. Stewart, David M. Boore, Kenneth W. Campbell, Mustafa Erdik, Walter Silva

Date: March 2013

Copyright © 2013 Jonathan P. Stewart, David M. Boore, Kenneth W. Campbell, Mustafa Erdik, Walter Silva. Except where otherwise noted, this work is made available under the terms of the [Creative Commons license CC BY 3.0 Unported](#)

The views and interpretations in this document are those of the individual author(s) and should not be attributed to the GEM Foundation. With them also lies the responsibility for the scientific and technical data presented. The authors do not guarantee that the information in this report is completely accurate.

Citation: Stewart, J.P., D. M. Boore, K. W. Campbell, M. Erdik, W. Silva (2013) Define a Consistent Strategy to Model Ground Motion: Site Effects in Parametric Ground Motion Models, report produced in context of GEM GMPE project, available from <http://www.nexus.globalquakemodel.org/gem-gmpes>



ABSTRACT

This report is a component of Task 1. Our objective is to identify protocols for evaluating the site parameters used in GMPEs from data that are available on a global scale. The underlying assumption of this work is that the GMPEs selected in Task 3 are to be applied in subsequent GEM applications on a regional, as opposed to site-specific, scale. As a result of the regional-scale application, measurements of the relevant site parameters will not be available at the vast majority of locations where ground motions are to be estimated. Our work fills this gap by recommending correlation relationships that can produce statistical estimates of site parameters (median, standard deviation) conditional on information such as geologic and topographic conditions that are available for all, or most, global regions.

Chapter 1 of this report reviews a number of candidate GMPEs with specific emphasis on the site parameters employed in the models. This work clearly establishes that V_{s30} is a required input parameter for global application. Basin depth is also a parameter used in some relations. Chapter 2 describes procedures for estimation of V_{s30} from information such as geologic and geotechnical site classifications, topographic metrics, and V_s profile data shallower than 30 m. Chapter 3 describes procedures for estimation of basin depth and provides recommendations for utilizing these parameters in the GMPEs that require it. Chapter 4 summarizes the principal recommendations of this report.

Keywords: GMPE, attenuation, site effects, hazard

ACKNOWLEDGEMENTS

This study was funded by the GEM Foundation as part of the Pacific Earthquake Engineering Research Center's (PEER's) Global GMPEs project. Any opinions, findings, and conclusions or recommendations expressed in this material are those of the authors and do not necessarily reflect those of the sponsors.

TABLE OF CONTENTS

	Page
ABSTRACT	ii
ACKNOWLEDGEMENTS	iii
TABLE OF CONTENTS	iv
LIST OF FIGURES	v
LIST OF TABLES	vii
1 Site Classification Methods in GMPEs	1
2 Estimate of V_{S30}	5
2.1 Estimation based on Surface Geological and Geotechnical Categories	5
2.2 Estimation based on Ground Slope.....	9
2.3 Estimation based on Terrain-based Categories	14
2.4 Estimation based on Velocity Profiles Shallower than 30 Meters	15
2.5 Discussion of Methods and Comparison.....	19
3 Estimation of Basin Depth	22
4 Summary and Conclusions	25
References	27

LIST OF FIGURES

	Page	
Figure 2.1	Variation of Vs30 with horizontal distance from rock. From Wills and Gutierrez [2008].....	7
Figure 2.2	Variation of Vs30 with ground slope within basins. From Wills and Gutierrez [2008].....	8
Figure 2.3	Map of Vs30 for southern California derived from surface geologic categories and slope-based model for young alluvium. From Wills and Gutierrez [2008].....	8
Figure 2.4	Histograms of Vs30 from measurements within Geomatrix site categories. Data form NGA-W2 site database.....	10
Figure 2.5	Correlations of measured Vs30 (m/sec) versis topographic slope (m/m) for (a) active tectonic and (b) stable continental regions. Color-coded polygons represent median Vs30 for different increments of ground slope. From Wald and Allen [2007].....	11
Figure 2.6	From Wald and Allen [2007]. Histograms of prediction residuals of Vs30 – slope correlation for slope measurements at 30 arc sec and 9 arc sec resolutions. The similarity of the histograms indicates no increase of predictive power when higher resolution topographic data is utilized. Modified from Allen and Wald [2009].....	12
Figure 2.7	Variation of slope, texture, and convexity with terrain categories of Yong <i>et al</i> [2011].....	14
Figure 2.8	Histograms of log Vs10 and log Vs20 for shear-wave velocity models from K-net, KiK-net, and California, for zp = 20 m. From Boore <i>et al</i> [2011].....	17
Figure 2.9	Histogram of ground slopes at sites in California and Japan from which the velocity models were obtained. From Boore <i>et al</i> [2011]	17
Figure 2.10	Comparison of Vs30-Vsz relationships developed by Yu and Silva and Boore <i>et al</i> [2011] for four profile depths, zp.....	18
Figure 2.11	Comparison of Vs30-Vsz relationships developed by Yu and Silva and Boore <i>et al</i> [2011] with Kiknet data for four profile depths, zp.....	19
Figure 2.12	Dispersion of Vs30 prediction residuals reported as natural log standard deviation ($\sigma_{\ln V}$). Results from Moss [2008] are COVs taken as approximately equal to $\sigma_{\ln V}$. Explanation of codes. Measurements: SW = surface wave methods, Intr = intrusive methods (borehole). Surface geology: M rock = Mesozoic rock categories, P, T = Pleistocene and Tertiary categories, Qi, Qa = Quaternary mud and alluvium categories. GMX: A-E, see Table 2.2. Terrain: numbered categories, see Table 2.4.	21
Figure 2.13	COV of Vs30 values estimated using geologic correlations by Wills and Clahan [2006]. From Moss [2008]	21
Figure 3.1	Trend of basin depth Z1.0 with Vs30 and fit models proposed by Abrahamson and Silva [2008] and Chiou and Youngs [2008a]. Data from NGA-West2 site database.....	23

- Figure 3.2** Trend of basin depth Z2.5 with (a) Vs30 and (b) depth Z1.0 along with fit model proposed Campbell and Bozorgnia [2007]..... 24

LIST OF TABLES

Table 1.1	Site parameters and site amplification information for GMPEs selected for Task 2 of GEM Global GMPEs project by Douglas <i>et al</i> [2011]	2
Table 1.2	NEHRP site categories.	3
Table 1.3	Site categories used for GMPE of Zhao <i>et al</i> [2006].....	3
Table 1.4	Site categories used in Eurocode, CEN [2004].....	4
Table 2.1	Geologic units and shear-wave velocity characteristics. Wills and Clahan [2006].	6
Table 2.2	Geomatrix site categories and statistics on Vs30. Data are from sites in NGA-W2 site database with Vs30 measurements.	9
Table 2.3	Correlations between topographic gradient and Vs30 using NED 9c DEMs for the NEHRP site classes. From Wald and Allen	13
Table 2.4	Terrain based categories by Yong <i>et al</i> [2011] and corresponding Vs30 statistics.	15

1 Site Classification Methods in GMPEs

In this paragraph, we identify the site parameters commonly utilized in ground motion prediction equations (GMPEs). We have not undertaken an independent review of GMPEs. Rather, we utilize the list of the GMPEs compiled in Task 2 of the GEM Global GMPEs project by Douglas *et al* [2011], and focus on the representation of site conditions within those models. Table 1.1 lists those GMPEs, describes the site parameters included in the models, and provides some details on the site amplification model. The GMPEs are organized by tectonic regime, with most being in stable continental regions, subduction zones, or active tectonic regions.

Table 1.1 distinguishes between site classification methods based on discrete categories or continuous variables. Discrete categories are most often described by the NEHRP criteria given in Table 1.2, which are defined on the basis of V_{s30} .

As shown in Table 1.3, Zhao *et al* [2006] utilize categories that can be defined from V_{s30} or site period, the latter of which is generally evaluated from the peak in H/V spectral ratios.

Table 1.4 lists the CEN [2004] categories used in Eurocode, which are closely related to NEHRP categories.

Several additional categorization schemes are used, as indicated in Table 1.1. Di Alessandro *et al* [2011] have recently proposed site categories defined from site period, similar to Zhao *et al* [2006], but which also allow for conditions where the H/V spectral ratios are relatively flat and hence do not identify a site period.

Site parameters defined as continuous variables include V_{s30} and parameters describing the depth to a shear wave isosurface (Z_x) having a velocity $V_s = x$ km/sec. Values of x that have been used to date are 1.0 km/sec and 2.5 km/sec. Chapters 2 and 3 describe procedures that can be used to estimate V_{s30} and depth parameters, respectively. We have not found any direct uses of site period as a continuous variable in GMPEs.

As shown in Table 1.1, most GMPEs utilize linear site terms, meaning that the site amplification is constant with respect to the amplitude of ground shaking. The reference site condition listed in Table 1.1 is the condition for which the site amplification is unity. This condition generally corresponds to rock site conditions.

Table 1.1 Site parameters and site amplification information for GMPEs selected for Task 2 of GEM Global GMPEs project by Douglas *et al* [2011]

	Reference	Application Region	Site Parameters		Site Amplification Function	
			Discrete categories ¹	Continuous Variables ²	Non-linearity	Reference site condition ³
Stable continental regions	Atkinson (2008), Atkinson & Boore (2011)	CEUS	NEHRP B/C only	-	na	NEHRP B/C
	Atkinson & Boore (2006, 2011)	CEUS	Hard rock; NEHRP B/C	V_{s30}	Yes	Hard rock ($V_s=2000$ m/s)
	Campbell (2003)	CEUS	Hard rock only	-	na	Hard rock ($V_s=2800$ m/s)
	Douglas <i>et al.</i> (2006)	So. Norway	Hard rock only	-	na	Hard rock ($V_s=2800$ m/s)
	Frankel <i>et al.</i> (1996)	CEUS	Hard rock; NEHRP B/C	-	na	Hard rock ($V_s=2800$ m/s)
	Raghuram & Iyengar (2006, 2007)	Peninsular India	Hard rock; NEHRP A-D	-	Yes	Hard rock ($V_s=3600$ m/s)
	Silva <i>et al.</i> (2002)	CEUS	Hard rock only	-	na	Mid-cont., $V_s=2830$ m/s; Gulf cst $V_s=2310$ m/s)
	Somerville <i>et al.</i> (2009)	Australia	Rock only	-	na	Rock ($V_s=1000$ m/s)
	Pezeshk <i>et al.</i> (2011)	CEUS	Hard rock only	-	na	Hard rock ($V_s>2000$ m/s)
	Toro <i>et al.</i> (1997)	CEUS	Hard rock only	-	na	Hard rock ($V_s=2800$ m/s)
Subduction zones	Atkinson & Boore (2003)	Global	NEHRP B-E	-	Yes	NEHRP B
	Atkinson & Macias (2009)	Cascadia	NEHRP B/C only	-	na	NEHRP B/C
	Garcia <i>et al.</i> (2005); Arroyo <i>et al.</i> (2010)	Mexico	NEHRP B only	-	na	NEHRP B
	Zhao <i>et al.</i> (2006); Zhao (2010)	Japan	Four: hard rock to soft soil	-	No	Not defined
	Kanno <i>et al.</i> (2006)	Japan	-	V_{s30}	No	$V_{s30} \approx 300$ m/s
	Lin & Lee (2008)	Taiwan	Two: rock & soil	-	Yes	Not defined
	McVerry <i>et al.</i> (2006)	New Zealand	Five: strong rock to v soft soil	-	Yes	Strong rock and rock
	Youngs <i>et al.</i> (1997)	Global	Three: GMX A, B, D	-	No	Not defined
	Abrahamson & Silva (2008)	Global	-	$V_{s30}, Z_{1.0}$	Yes	$V_{s30}=1100$ m/s
Active tectonic regions	Akkar & Bommer (2010)	Europe & Middle East	Two: rock, stiff & soft soil	-	No	Rock
	Boore & Atkinson (2008, 2011)	Global	-	V_{s30}	Yes	$V_{s30}=760$ m/s
	Campbell & Bozorgnia (2008)	Global	-	$V_{s30}, Z_{2.5}$	Yes	$V_{s30}=1100$ m/s
	Cauzzi & Faccioli (2008); Faccioli <i>et al.</i> (2010)	Global	CEN A-D	V_{s30}	No	CEN A
	Chiou & Youngs (2008)	Global	-	$V_{s30}, Z_{1.0}$	Yes	$V_{s30}=1130$ m/s
	Kanno <i>et al.</i> (2006)	Japan	-	V_{s30}	No	$V_{s30} \approx 300$ m/s
	McVerry <i>et al.</i> (2006)	New Zealand	Five: strong rock to v soft soil	-	Yes	Strong rock and rock
	Zhao <i>et al.</i> (2006)	Japan	Four: hard rock to soft soil	-	No	Not defined
	McVerry <i>et al.</i> 2006	New Zealand	Five: strong rock to v soft soil	-	Yes	Strong rock and rock
Volcanic regions	Zhao (2010)	Japan	Four: hard rock to soft soil	-	No	Not defined
	Sokolov <i>et al.</i> 2008	Romania	Hard rock only	-	No	Hard rock ($V_s = 3800$ m/s)

¹ NEHRP categories in Table 2.2; Zhao *et al.* (2006) categories in Table 2.3; GMX categories (used by Youngs *et al.*, 1997) in Table 3.2; CEN categories in Table 2.4

² V_{s30} from Eq. 3.1 with $z_p = 30$ m; V_{su} is determined over undefined depth.

³ Reference site condition defined as having no site modification in the GMPE. 'Not defined' indicates separate regression coefficients evaluated for different site conditions (no specific site term)

Table 1.2 NEHRP site categories.

Class	V_{30} Range (m/sec)	Profile Type
A	> 1500	Hard rock
B	760–1500	Rock
C	360–760	Very dense soil/soft rock
D	180–360	Stiff soil
E	< 180	Soft soil
F	Special soils requiring site-specific evaluation	

Table 1.3 Site categories used for GMPE of Zhao *et al* [2006].

Site class	Description	Natural Period	V_{30} Calculated from Site Period	NEHRP Site Classes
Hard rock			$V_{30} > 1100$	A
SC I	Rock	$T < 0.2$ sec	$V_{30} > 600$	A+B
SC II	Hard soil	$0.2 = T < 0.4$ sec	$300 < V_{30} = 600$	C
SC III	Medium soil	$0.4 = T < 0.6$ sec	$200 < V_{30} = 300$	D
SC IV	Soft soil	$T = 0.6$ sec	$V_{30} = 200$	E+F

Table 1.4 Site categories used in Eurocode, CEN [2004].

Site Class	Profile Type	V_{530} (m/sec)
A	Rock of other rock-like geological formation, including at most 5 m of weaker material at the surface	> 800
B	Deposits of very dense sand, gravel, or very stiff clay, at least several tens of metres in thickness, characterized by a gradual increase of mechanical properties with depth.	360–800
C	Deep deposits of dense of medium-dense sand, gravel, or stiff clay with thicknesses from several tens to man hundreds of metres.	180–360
D	Deposits of loose-to-medium cohesionless soil (with or without some soft cohesive layers), or of predominately soft-to-firm cohesive soil.	< 180
E	A soil profile consisting of a surface alluvium layer with Vs values of type C or D, and thickness varying between about 5 m and 20 m, underlain by stiffer material with Vs > 800 m/sec.	
S1	Deposits consisting of, or containing, a layer at least 10 m thick, of soft clays/silts with a high plasticity index ($PI > 40$) and a high water content.	< 100 (indicative)
S2	Deposits of liquefiable soils, of sensitive clays, or any other soil profile not included in Types A-E or S1	

2 Estimate of V_{s30}

2.1 Estimation based on Surface Geological and Geotechnical Categories

Correlations have been developed to link surface geologic units and geotechnical categories to V_{s30} . Some of these correlations are well documented and based on large inventories of V_s profiles; these tend to be based on surface geology. The correlations for geotechnical categories tend to be relatively poorly documented and often use proprietary data sets of various sizes. In this section, we emphasize the surface geologic correlations, but also provide the correlations for geotechnical categories that were used in the original NGA project.

Wills and Clahan [2006] prepared correlation relationships between surface geology and V_{s30} and prepared maps for portions of California based on those relationships. The profile database used by Wills and Clahan (WC) was from PEA, consisting of 556 profiles. A key consideration in developing the WC relationship was variations of velocities within the broad geological categories typically shown in geological maps (e.g., Quaternary alluvium, Qa). For example, young alluvial deposits are rarely 30 m thick, so V_{s30} is influenced by underlying material that will generally be older and faster. This motivated discretization of alluvial categories to separate thin and deep Qa. In addition, regional conditions cause some alluvial basins, such as the Imperial Valley and Los Angeles basins, to have somewhat distinct velocities relative to the overall averages for Qa. As shown in Table B.5, to capture these features, WC divide young alluvium into eight categories: Qal, fine; Qal, deep; Qal, deep, Imperial V; Qal, deep, LA Basin; Qal, thin; Qal, thin, west LA; and Qal, coarse. These categories represent in an approximate way the general velocity gradient in alluvial basins away from mountain fronts and regional variations in velocity structure.

In total, 19 generalized geologic units were specified for California as shown in Table 2.1. For each unit WC present mean and standard deviations of V_{s30} and $\ln(V_{s30})$ (the later anticipating a log normal distribution of velocities). Composite profiles were also presented for each unit, which typically extend below 30 m in depth. WC used the largest-scale geological maps available to them in their work (e.g., 1:24,000), and applications of the correlations should ideally use maps with similar levels of resolution.

WC prepared a site conditions map on basis of the units from Table 2.1, but it was incomplete at the time of publication in 2006. The map was subsequently completed by Wills and Gutierrez [2008] (WG).

WG also extended the earlier work by developing more systematic and quantitative guidelines for distinguishing variable conditions within Qa. For example, distinguishing ‘Qal,thin’ from ‘Qal,deep’ was largely a judgment-driven process in the WC work, which complicates application elsewhere by different investigators. Two methods of distinguishing ground conditions within Qa were examined

Table 2.1: Geologic units and shear-wave velocity characteristics. Wills and Clahan [2006].

Geologic Unit	Geologic Description	No. of profiles	Mean V_{s30}	S.D.	V_{s30} from Mean of In	$\sigma_{\ln V}$
Qi	Intertidal Mud, including mud around the San Francisco Bay and similar mud in the Sacramento/San Joaquin delta and in Humboldt Bay	20	160	39	155	0.243
af/qi	Artificial fill over intertidal mud around San Francisco Bay	44	217	94	202	0.357
Qal, fine	Quaternary (Holocene) Alluvium in areas where it is known to be predominantly fine	13	236	55	229	0.238
Qal, deep	Quaternary (Holocene) Alluvium in areas where the alluvium (Holocene and Pleistocene) is more than 30 m thick; generally much more in deep basins	161	280	74	271	0.250
Qal, deep,Imp V	Quaternary (Holocene) alluvium in the Imperial Valley, except sites in the northern Coachella Valley adjacent to the mountain front	53	209	31	207	0.135
Qal, deep, LA Basin	Quaternary (Holocene) alluvium in the Los Angeles basin , exect sites adjacemt to the mountain fronts	64	281	85	270	0.275
Qal, thin	Quaternary (Holocene) alluvium in narrow valleys, small basins , and adjacent to the edges of basins where the alluvium would be expected to be underlain by contrasting material within 30 m	65	349	89	338	0.244
Qal, thin, west LA	Quaternary (Holocene) alluvium in part of west Los Angeles where the Holocene alluvium is know to be thin, and is underlain by Pleistocene alluvium	41	297	45	294	0.150
Qal, coarse	Quaternary (Holocene) alluvium near fronts of high steep mountain ranges and in major channels where athe alluvium is expected to be coarse	18	354	82	345	0.223
Qoa	Quaternary (Pleistocene) alluvium	132	387	142	370	0.273
Qs	Quaternary (Pleistocene) sand deposits, such as the Merritt Sand in the Oakland larea	15	302	46	297	0.171
QT	Quaternary to Tertiary (Pleistocene-Pliocene) alluvial deposits such as athe Saugus Formation of southern California, Paso Robles Formation of central cost ranges, and the Santa Clara Formation of the Bay Area	18	455	150	438	0.266
Tsh	Tertiary (mostly Miocene and Piocene)shale and siltstone units such as the Repetto, Fernando, Puente, and Modelo Formations of the Los Angeles area	55	390	112	376	0.272
Tss	Tertiary (mostly Miocene, Oligocene , and Eocene) sandstone units such as the Topanga Formation in Los Angeles area and the Butano sandstone in in the San Francisco Bay area	24	515	215	477	0.386
Tv	Tertiary volcanic units including the Conejo Volcanics in the Santa Monica Mountais and the Leona Rhyolite in East Bay Hills	3	609	155	597	0.24
Kss	Cretaceous sandstone of the Great Valley Sequence in central Coast Ranges	6	566	199	539	0.332
searpentine	Serpentine, generally considered part of the Franciscan complex	6	653	137	641	0.204
KJf	Franciscan complex rock , including melange , sandstone, shale, chert, and greenstone	32	782	359	712	0.432
xtaline	Crystalline rocks, including Cretaceous granitic rock , Jurassic metmorphic rocks, schist , and Precambrian gneiss	28	748	430	660	0.489

1. Effect of horizontal distance from rock, defined as Tertiary sandstone and shale, Franciscan and other Cretaceous rocks, and all metamorphic, volcanic and plutonic rocks. Older alluvium and Plio-Pleistocene categories (Qoa, Qs, and QT) were not included as “rock”.
2. Effect of ground slope, measured from digital elevation models. WG point out that their ground slope correlations apply to Qa only (depositional areas) and hence would not be expected to be applicable to bedrock environments (typically erosional areas).

As shown in Figure 2.1, the ground slope correlation shows decreasing velocity with distance from rock up to a distance of 10 km. This follows expected patterns, as stream power is relatively high near basin edges, causing sediments in those areas to be relatively coarse (hence fast), whereas mid-basin areas have finer-grained alluvium. Moreover, basin edge areas tend to have thin alluvium.

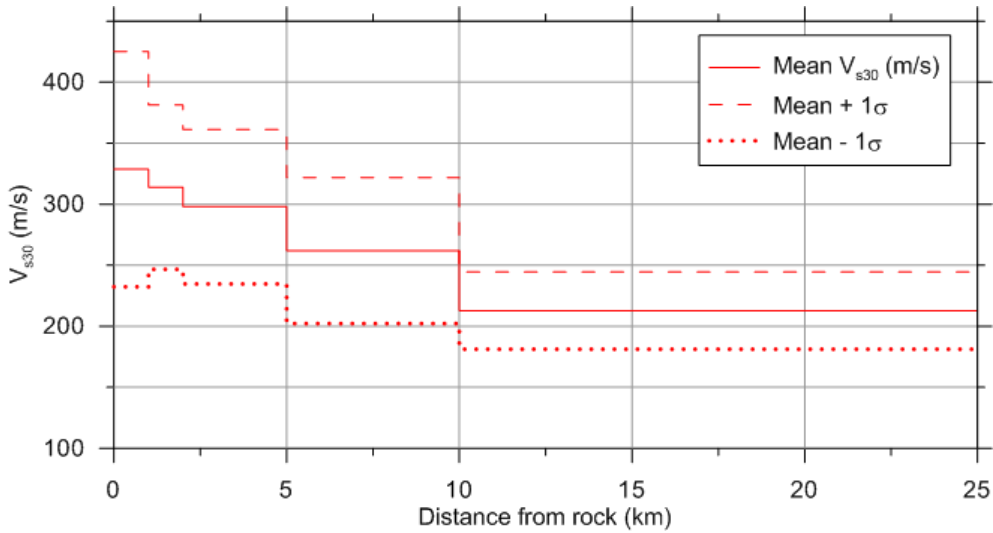


Figure 2.1 Variation of V_{s30} with horizontal distance from rock. From Wills and Gutierrez [2008].

Figure 2.2 similarly shows an increase of velocity with slope, which also follows expected trends. Both Figures 2.1 and 2.2 also show that the standard deviation of velocities decrease as the V_{s30} decreases (i.e., for increasing distance from rock and flatter slopes). Figure 2.3 shows a velocity map for southern California in which the slope-based model is used within basins and the WC velocities are used elsewhere.

The WC and WG correlations are based on geologic conditions and V_s profiles in California. The applicability of the WC correlations to Italy was investigated by Scasserra *et al* [2009], who found that the median velocities for WC Quaternary categories (including the Qa categories and Qoa, Qs, and QT) are unbiased relative to Italian data. The applicability of the WC model to other regions is unknown.

The principal geotechnical site categorization scheme that has been used in previous ground motion studies and correlated to V_{s30} , including NGA, is attributed to the former consulting firm Geomatrix (GMX). The GMX scheme has three letters, the last of which represents site condition. The GMX third letters and the corresponding site conditions are shown in Table 2.1. Using a site database for the NGA-West2 project [1] (i.e., a database of sites that have produced usable recordings), we have identified 470 sites with both GMX third letter classifications and V_{s30} values based on measurements. We use data from sites with geophysical measurements to depths $z > 20$ m. For sites with $z = 20\text{--}29$ m, we use the Boore [2004] extrapolation technique described in Section 3.4. Histograms of V_{s30} for each site category are shown in Figure 2.4, in which median and standard deviations are identified. Those values are also shown in Table 2.2, and provide a basis for estimation of V_{s30} when Geomatrix site classifications have been assigned. The results shown in Table 2.2

are very similar to unpublished results developed for the original NGA project [Chiou and Youngs 2008b; Silva and Darragh, 2011, *personal communication*].

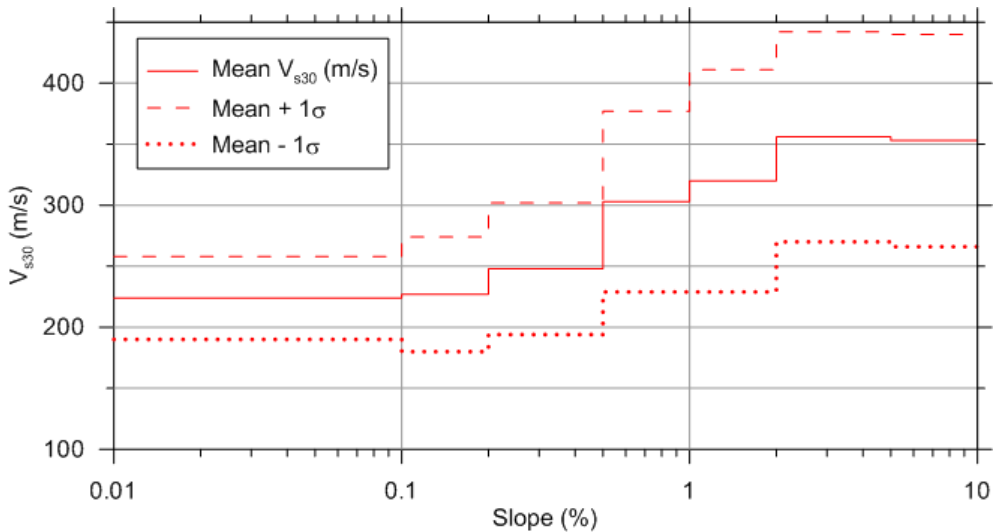


Figure 2.2 Variation of Vs30 with ground slope within basins. From Wills and Gutierrez [2008].

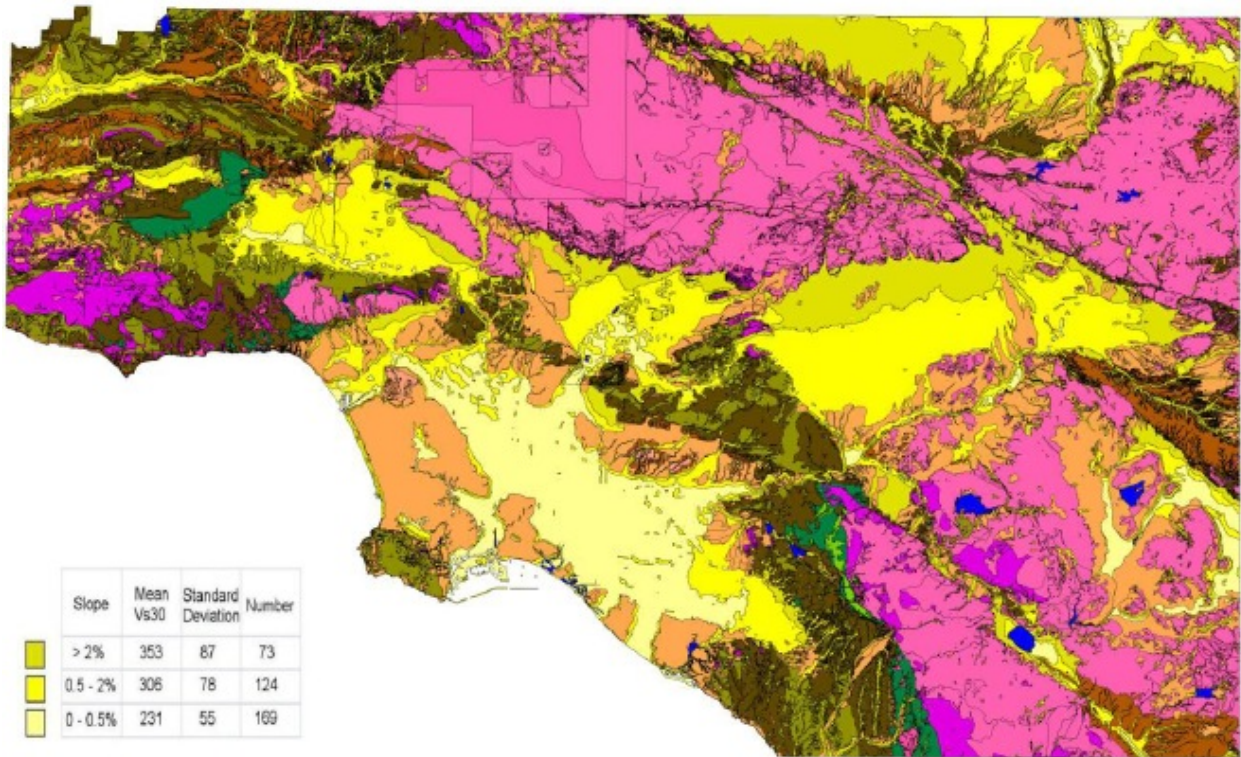


Figure 2.3 Map of Vs30 for southern California derived from surface geologic categories and slope-based model for young alluvium. From Wills and Gutierrez [2008].

Table 2.2: Geomatrix site categories and statistics on Vs30. Data are from sites in NGA-W2 site database with Vs30 measurements.

Geomatrix	Third Letter	Description	Median		Mean V_{s30} (m/sec)	σ
			V_{s30} (m/sec)	σ_{ln}		
A	Rock. Instrument on rock ($V_s > 600$ mps)		673	0.43	700	365
B	Shallow (stiff) soil. Instrument on/in soil profile up to 20 m thick overlying rock.		439	0.35	487	142
C	Deep narrow soil. Instrument on/in soil profile at least 20 m thick overlying rock, in a narrow canyon or valley no more than several km wide		331	0.25	356	87
D	Deep broad soil. Instrument on/in soil profile at least 20 m thick overlying rock, in a broad valley		266	0.34	298	110
E	Soft deep soil. Instrument on/in deep soil profile with average $V_s < 150$ mps)		192	0.27	194	61

2.2 Estimation based on Ground Slope

Correlations have been developed to link surface topographic features to V_{s30} . The most well-known of these correlations relates topographic slope to V_{s30} [Wald and Allen, 2007; Allen and Wald, 2009]. Another emerging technique categorizes surface topography according to various features (convexity, roughness, slope, etc.) and then correlates V_{s30} to those terrain based categories [Yong *et al*, 2011]. Another technique that has been used locally for Taiwan stations correlates V_{s30} to elevation [Chiou and Youngs, 2008b]. We describe here the basis for the ground slope technique and comment on its possible application. The terrain-based technique is discussed in Section 2.3.

The motivation behind development of the V_{s30} – slope correlation is that topographic data are globally available and slope can be anticipated to be an indicator of near-surface morphology and lithology [2].

Steep terrain is expected in mountains, indicating rock, whereas nearly flat slopes occur in basins, indicating soil. Transition zones would be expected to have moderate slopes involving weathered rock and potentially older sediments near basin boundaries.

Wald and Allen [2007] developed a correlation between ground slope and measured V_{s30} from invasive and non-invasive methods. The velocity data were compiled from active tectonic regions (California, Taiwan, Italy) and mid-plate regions (eastern US, Australia). At each location of a velocity measurement, ground slope was determined from global SRTM 30 arc sec (1-km spatial resolution) topographic data [Farr and Kobrick, 2000].

As shown in Figure 2.5, separate slope-Vs30 correlations were developed for active regions and mid-plate regions. Figure 2.5 shows that Vs30 increases with topographic slope indicating faster velocities for materials

on steeper slopes. Data exists for gradients < 7%, corresponding to a 4 degree slope. Equations relating Vs30 to slope were not provided; rather, stepped relationships of slope tied to discrete velocity bands were provided. Elevation was found to not provide additional predictive power for Vs30 beyond ground slope.

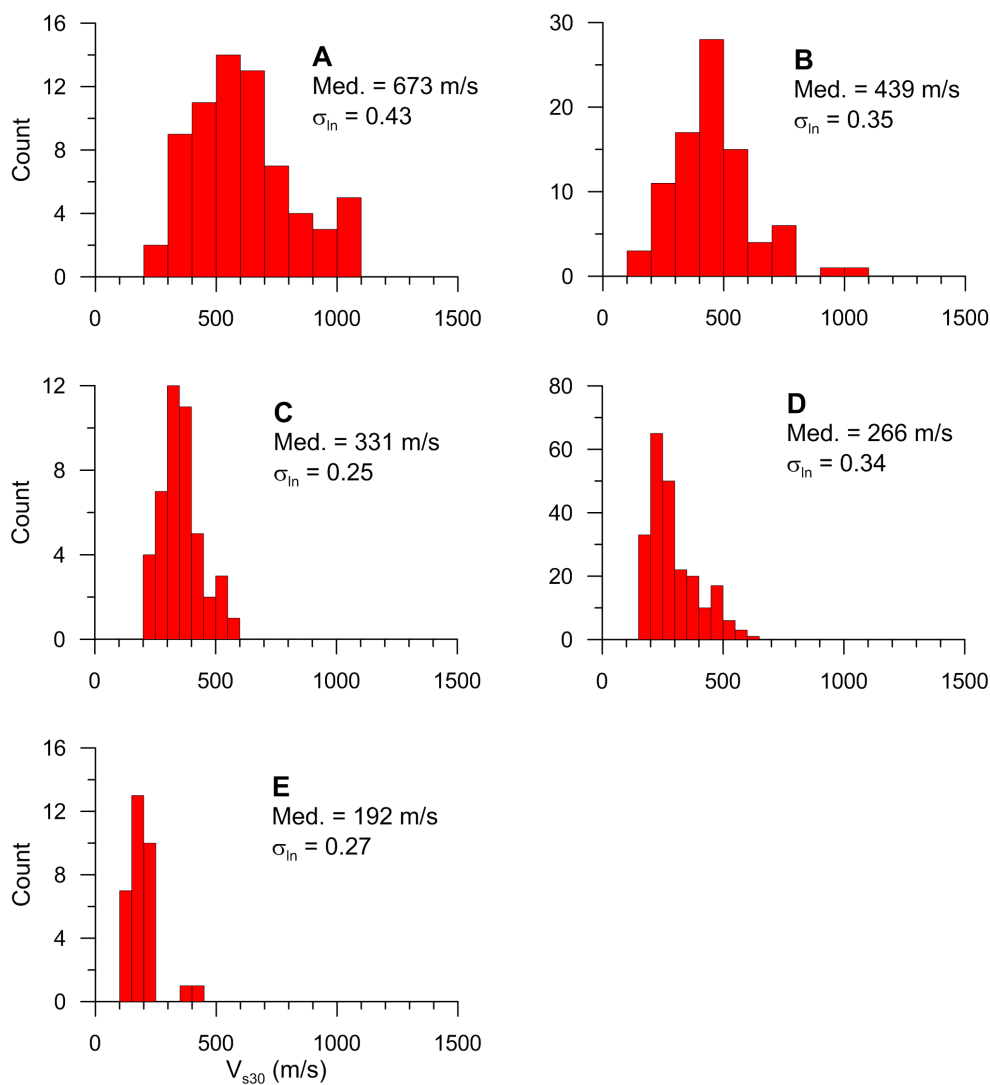


Figure 2.4 Histograms of Vs30 from measurements within Geomatix site categories. Data from NGA-W2 site database.

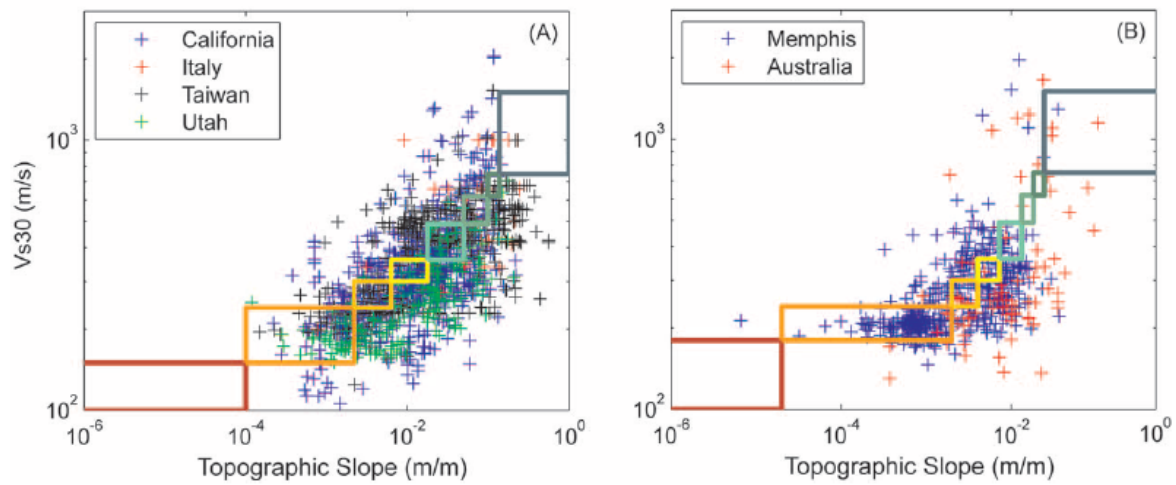


Figure 2.5 Correlations of measured Vs30 (m/sec) versus topographic slope (m/m) for (a) active tectonic and (b) stable continental regions. Color-coded polygons represent median Vs30 for different increments of ground slope. From Wald and Allen [2007].

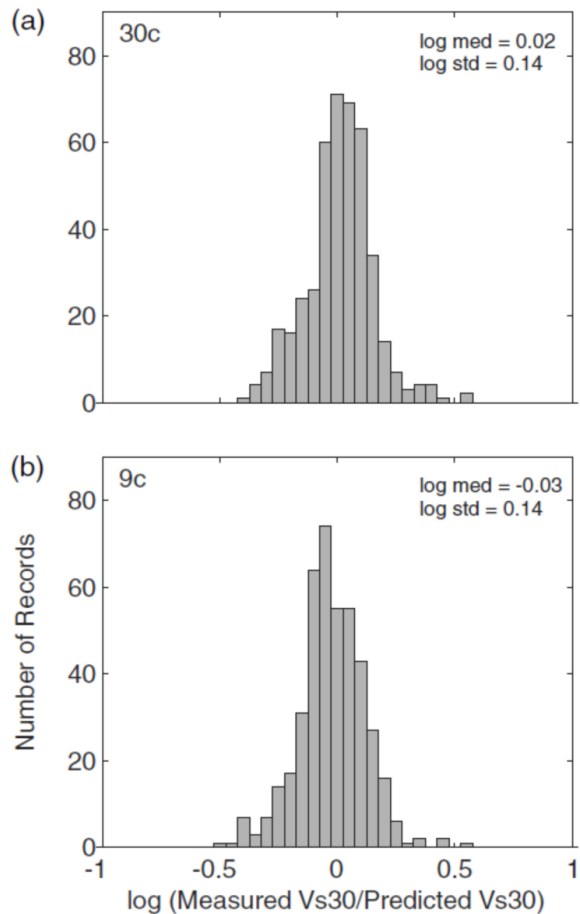


Figure 2.6 From Wald and Allen [2007]. Histograms of prediction residuals of Vs30 – slope correlation for slope measurements at 30 arc sec and 9 arc sec resolutions. The similarity of the histograms indicates no increase of predictive power when higher resolution topographic data is utilized. Modified from Allen and Wald [2009].

Table 2.3: Correlations between topographic gradient and Vs30 using NED 9c DEMs for the NEHRP site classes. From Wald and Allen

NEHRP Site Class	V _{s30} Range (m/sec)	9 arcsec Gradient Range (m/m) (Active Tectonic)	9 arcsec Gradient Range (m/m) (Stable Continent)	Modified 30 arcsec Gradient Range (m/m) (Active Tectonic)	30 arcsec Gradient Range (m/m) (Stable Continent)
E	> 180	> 3*10 ⁻⁴	> 1*10 ⁻⁴	> 3*10 ⁻⁴	> 2*10 ⁻⁵
	180–240	3*10 ⁻⁴ –3.5*10 ⁻³	1*10 ⁻⁴ –8.5*10 ⁻³	3*10 ⁻⁴ –3.5*10 ⁻³	2*10 ⁻⁵ –2*10 ⁻³
D	240–300	3.5*10 ⁻³ –0.010	4.5*10 ⁻³ –8.5*10 ⁻³	3.5*10 ⁻³ –0.010	2*10 ⁻⁵ –4*10 ⁻³
	300–360	0.010–0.024	8.5*10 ⁻³ –0.013	0.010–0.018	4*10 ⁻³ –7.2*10 ⁻³
C	360–490	0.024–0.08	0.013–0.022	0.018–0.05	7.2*10 ⁻³ –0.013
	490–620	0.08–0.14	0.022–0.03	0.05–0.10	0.013–0.018
B	620–760	0.14–0.20	0.03–0.04	0.10–0.14	0.018–0.025
	> 760	> 0.20	> 0.40	> 0.14	> 0.025

Allen and Wald [2009] utilize higher-resolution (3 and 9 arc sec) DEMs to examine whether V_{s30} can be resolved in more detail than with the lower-resolution SRTM data utilized by Wald and Allen [2007].

These higher resolution maps are not globally available, but are available for the United States through a USGS server. Allen and Wald find that higher resolution topographic data produces more resolution in slope maps that is useful to resolve features otherwise obscured at the 30 arc sec scale.

However, as shown in Figure 2.6, the increase of resolution from 30 arc sec to 9 arc sec does not appreciably affect histograms of V_{s30} residuals. This implies that increased topographic resolution does not improve V_{s30} estimates.

Allen and Wald's analysis of velocity data indicated biased V_{s30} predictions from the original Wald and Allen [2007] correlations for sites with steep gradients identified from higher-resolution topographic data. These resolution effects were not significant at lower gradients, although a V_{s30} overprediction bias was found for sites measured on low gradients. Accordingly, revised correlations were developed for the 30 arc sec data (active regions) and new correlations were developed for 9 arc sec data. The 30 arc sec correlations for stable regions were not changed from those of Wald and Allen [2007]. The currently recommended correlations are shown in Table 2.3.

There is some evidence of regional variations that may introduce bias in V_{s30} estimates made using these slope correlations; e.g., Wald and Allen [2007] comment on misfits of data gathered from Utah and Yu and Silva [2011, personal communication] found misfits for stations that recorded the Wenchuan, China earthquake. In some areas where detailed studies have been undertaken, a lack of correlation between V_{s30} and slope has been found (Santiago, Chile, Pilz *et al.* [2010]), while in other areas a correlation has been confirmed (Japan, Iwahashi *et al.*, [2010]; Parkfield, Thompson *et al.*, [2011]). Additional applications of this method outside of the original study regions include Romania [Bose *et al.*, 2009] and Hawaii [Atkinson, 2008].

2.3 Estimation based on Terrain-based Categories

The Yong *et al* [2011] procedure for V_{s30} estimation builds upon the slope-based correlations described in Section 2.2 to consider additional geomorphological factors including convexity and texture. This technique utilizes the same globally available SRTM 30 arc sec surface models employed by Wald and Allen [2007]. Hence, for a given location (latitude, longitude), the slope parameters used in the two models should be identical. The convexity element of the classification scheme is intended to distinguish convex-upward topography (characteristic of lowland terraces and alluvial fans) from concave-downward topography (broad valleys and foothills). The texture elements distinguish relatively smooth terrain from terrain having pits and peaks. These textural descriptions should not be confused with soil texture (e.g., fine, course) used in some sediment classification schemes (e.g., Fumal and Tinsley, [1985]).

Ground slope, convexity, and texture are jointly analyzed using an automated topography classification scheme by Iwashashi and Pike [2007] to segregate terrain types into 16 categories, which are listed in Table 2.4. A graphical representation of the classification scheme is given in Figure 2.7. As one moves to the right in the matrix ground slope is decreasing, whereas moving down in the matrix produces less convexity and smoother texture. We note that the classification scheme has relatively fine discretization of rock conditions (rock categories include 1-7, 9, 11, and 13) but limited discretization of soil (e.g., there is no category that would seem to encompass lacustrine or marine clays, which produce the largest site amplification). This is a potential limitation of the procedure for site amplification studies, but one that could be easily corrected with an additional category.

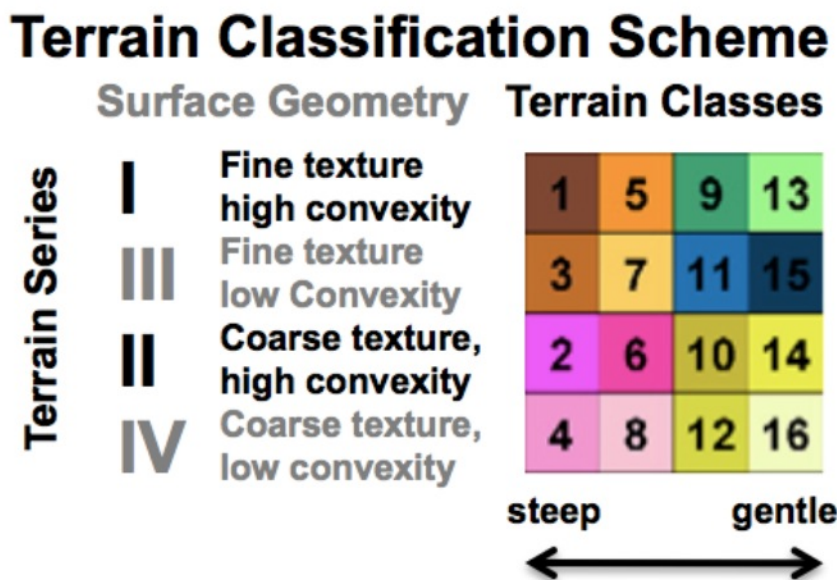


Figure 2.7 Variation of slope, texture, and convexity with terrain categories of Yong *et al* [2011].

Yong *et al* [2011] compiled 853 V_{s30} values from California prepared histograms of V_{s30} within each category, and compute category means as given in Table 2.4. The V_{s30} values used in the analysis included 209 from geophysical measurements and 644 (75%) from Wills and Clahan [2006] geology-based correlation, as described in Section 2.1. Because most of the data are from WC correlations, this classification scheme is not independent of the geology-based scheme. It should be noted that some of the categories are very sparsely populated with V_{s30} data, including 2, 6, 9, 10, 13, 14, and 15.

Using the NGA-W2 site database, we have identified 210 sites in California with V_{s30} values based on measurements. At our request, Alan Yong (*personal communication*, [2011]) provided terrain-based categories (using the scheme described in Table 2.4), and on that basis we have estimated V_{s30} values and calculated residuals and their intra-category means and standard deviations. California sites were used to expedite the calculations; a more comprehensive analysis using data from other regions will be undertaken at a later date. The number of measurements within the categories is shown in Table 2.4 along with the log mean (μ_{Inv}) and standard deviation of residuals (σ_{Inv}).

Most categories have slightly negative mean residuals, indicate model overprediction. The well-populated soil categories (8, 12, 16) have markedly lower dispersion than well-populated rock categories (1, 3, 4, 7).

Application of the Yong *et al* [2011] scheme involves determining the classification of a site of interest using the SRTM data with the Iwahashi and Pike [2007] procedure [3]. The V_{s30} value is then read from Table 2.4 along with its corresponding uncertainty. Because the V_{s30} data is entirely from California, the applicability of this technique to other regions is unknown. A similar technique has been applied to Mozambique, Pakistan and Turkey [Yong *et al*, 2008a, 2008b].

Table 2.4: Terrain based categories by Yong *et al* [2011] and corresponding Vs30 statistics.

Category Description	From Yong et al. 2011			This study		
	Freq. in CA (%)	Mean V_{s30} (m/s)	# V_{s30} meas.	μ_{Inv}	σ_{Inv}	
1 Well dissected mountains, summits, etc.	21	519	19	-0.12	0.41	
2 Large volcanoe, high block plateaus, etc.	2	393	1			
3 Well dissected, low mountains, etc.	14	547	25	-0.06	0.59	
4 Volcanic fan, foot slope of high block plateau, etc.	19	459	24	0.10	0.45	
5 Dissected plateaus, etc.	6	402	8			
6 Basalt lava plain, glaciated plateau, etc.	1	345	0			
7 Moderately eroded mountains, lava flow, etc.	7	388	25	-0.10	0.53	
8 Desert alluvial slope, volcanic fan, etc.	12	374	41	-0.06	0.32	
9 Well eroded plain of weak rocks, etc.	1	497	2			
10 Valley, till plain, etc.	<1	349	1			
11 Eroded plain of weak rocks, etc.	2	328	9			
12 Desert plain, delta plain, etc.	4	297	16	-0.10	0.21	
13 Incised terrace, etc.	<1	--	0			
14 Eroded alluvial fan, till plain, etc.	<1	209	1			
15 Dune, incised terrace, etc.	1	363	2			
16 Fluvial plain, alluvial fan, low lying flat plains, etc.	8	246	36	-0.18	0.18	

2.4 Estimation based on Velocity Profiles Shallower than 30 Meters

It is not unusual for shear-wave velocities to extend to depths shallower than 30 m. In such cases, V_{s30} cannot be calculated directly, but the available geophysical data to profile depth z_p can be used to estimate V_{s30} . The average velocity to depth z_p , termed V_{sz} , is calculated similarly to V_{s30} :

$$V_{sz} = \frac{z_p}{\Delta t_z} \quad (2.1)$$

Where z_p = profile depth and Δt_z = travel time for shear waves from depth z_p to the ground surface, calculated as:

$$\Delta t_z = \int_0^{z_p} \frac{dz}{V_s(z)} \quad (2.1)$$

Using these variables, the procedures under discussion in this section are intended to estimate V_{s30} from V_{sz} conditional on z_p .

The simplest method to estimate V_{s30} from V_{sz} for $z_p < 30$ m is to extend the lowermost velocity in the profile to 30 m [Boore, 2004]. This procedure was used for Vs30 calculation for the NGA database [Chiou *et al*, 2008] for sizes with $20 < z_p < 30$ m. More generally, correlation relationships are used based on borehole measurements in similar terrains. Boore [2004] used profile data from 135 boreholes in California to develop V_{s30} - V_{sz} correlations. Kanno *et al* [2006], Cauzzi and Faccioli [2008], Cadet and Duval [2009], and Boore *et al* [2011] utilized velocity profiles based on borehole measurements at 691 vertical array sites in Japan that are within the KiK-net network [Kinoshita, 1998; Okada *et al*, 2004]. As described by Boore *et al* [2011], the KiK-net sites are preferentially located on relatively hard rock geologic conditions, so V_{s30} - V_{sz} correlation relationships will reflect that type of geology, even though some Kiknet stations are at soil sites.

An expression for relating V_{sz} to V_{s30} is:

$$\log(V_{s30}) = c_0 + c_1 \log(V_{sz}) + c_2 [\log(V_{sz})]^2 \quad (2.3)$$

where c_0 , c_1 , and c_2 are regression coefficients that depend on profile depth z_p . Boore [2004] use a linear model (i.e., $c_2=0$) and provide coefficients for $z_p=10$ to 29 m. Boore *et al* [2011] find that the Boore [2004] model is effective for alluvial and soft rock geologies outside California, including the K-net sites in Japan (typically located on sediments in urban areas), Turkey, and locations in Europe. This is illustrated in Figure 2.8 (right side), which shows V_{s20} values for K-net sites that are similar to those for California sites. However, Boore *et al* [2011] find the 2004 model is biased for Kiknet sites (generally having stiffer rock conditions) and develop an alternative relationship using the 2nd order polynomial form in Eq. (2.3) for depths ranging from 5 to 29 m using the KiK-net data. Figure 2.8 (left side) illustrates this bias, by the shift towards faster V_{s20} values for KiK-net sites relative to K-net sites.

These differences in velocities are consistent with a statement by Okada *et al* [2004] that K-net and KiK-net stations are predominantly located on soil and rock sites, respectively. The KiK-net stations in Japan are located on a nominally uniform grid, which means that a number of stations are in valleys in hilly terrain with shallow sediments over rock. California stations are predominately in urban areas, such as the Los Angeles and San Francisco, which are located within broad areas of low topographic relief, underlain by sedimentary basins. Figure 2.9 shows histograms of topographic slopes for California strong motion sites and Japan KiK-net sites. The slopes at the California borehole sites are systematically lower than those at the KiK-net sites in Japan indicating the tendency to be sited on stiffer soils or rock in Japan.

Yu and Silva (*pers. communication*, R. Darragh, [2011]) also noted bias in the Boore [2004] V_{s30} - V_{sz} correlations during a PEER study of Vs data from 147 sites in southwest China (SWC sites) that recorded the Wenchuan, China earthquake. This bias was identified by calculating V_{s30} at the SWC sites by extending the lowermost velocity in the profile to 30 m (simple extrapolation) and then comparing those results to estimates from Boore [2004], from which an under-prediction bias of 0.139(ln) was found for 32 sites with $z_p = 10$ -20 m. Elevation and terrain proxies for V_{s30} also had significant bias for those sites.

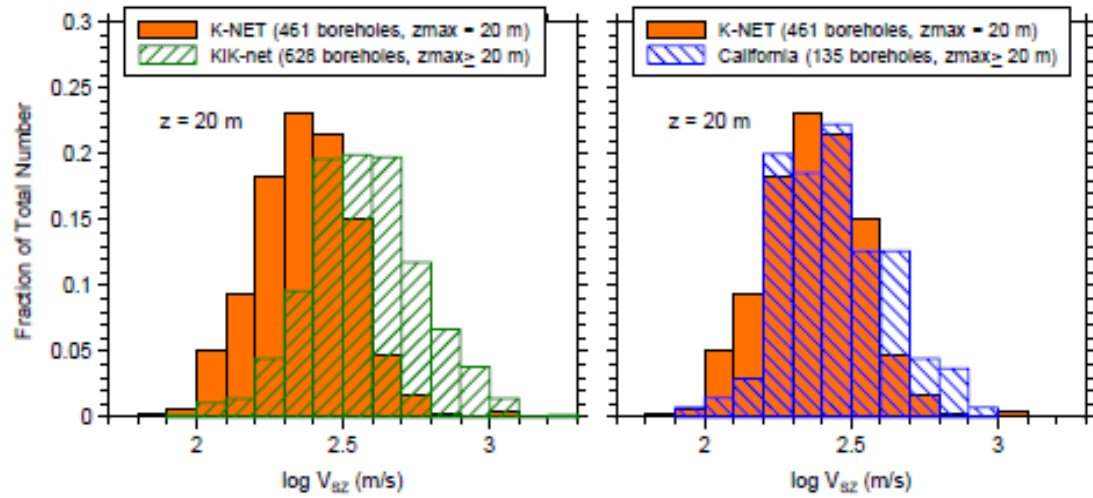


Figure 2.8 Histograms of log Vs₁₀ and log Vs₂₀ for shear-wave velocity models from K-Net, KiK-Net, and California, for $z_p = 20$ m. From Boore *et al* [2011].

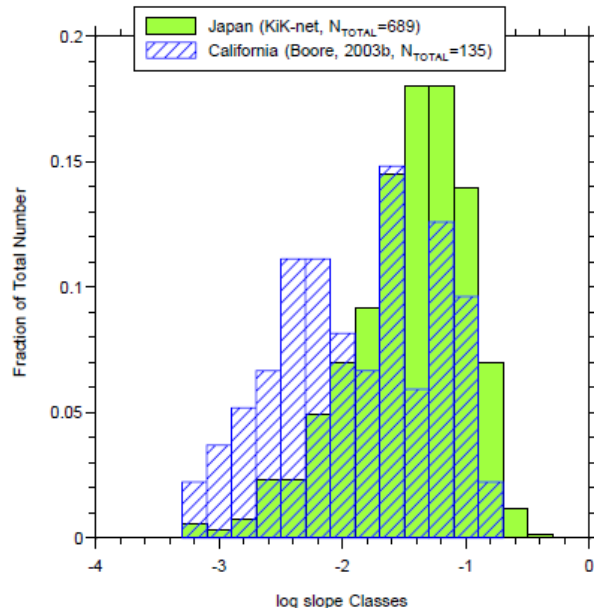


Figure 2.9 Histogram of ground slopes at sites in California and Japan from which the velocity models were obtained. From Boore *et al* [2011].

Yu and Silva's finding of bias led to the development of V_{s30} - V_{sz} correlations using sites generally stiffer than California [Boore, 2004] as the Boore *et al* [2011] analyses were not available. A V_{s30} - V_{sz} relationship was derived from 73 selected Kik-Net sites having GMX third letter classifications using both linear ($c_2=0$) and parabolic equations (it was not possible for this relationship to be based on SWC data because very few of those boreholes extend beyond 30 m). A linear relationship was recommended that is not conditioned on additional parameters such as GMX site codes. The Yu and Silva correlations were not intended to replace the Boore *et al* [2011] correlations and were intended to address only the SWC recording stations.

Figure 2.10 compares the V_{s30} - V_{sz} correlations from Boore *et al* [2011] and Yu and Silva [2011]. The differences between the curves increase as z_p decreases, with the Silva and Yu model having a flatter gradient for $z_p = 5$ and 10 m (leading to higher V_{s30} estimates for low V_{sz} ; lower V_{s30} for high V_{sz}). The

differences between the curves are minor for $V_{sz} > 250$ m/sec, which is a common condition for SWC sites (the target application region for Yu and Silva). Figure 2.11 compares the two correlations to Kiknet data for four values of z_p . The Boore *et al* parabolic model generally provides a better fit, although the difference is most significant for $V_{sz} < 200$ m/sec.

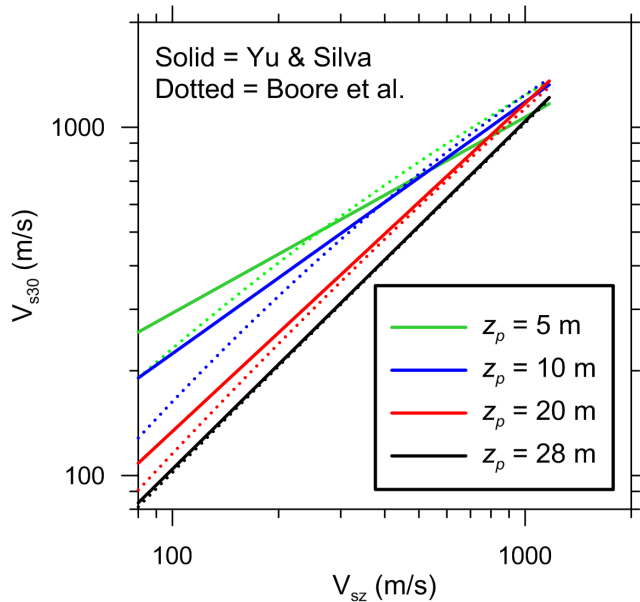


Figure 2.10 Comparison of V_{s30} - V_{sz} relationships developed by Yu and Silva and Boore *et al* [2011] for four profile depths, z_p .

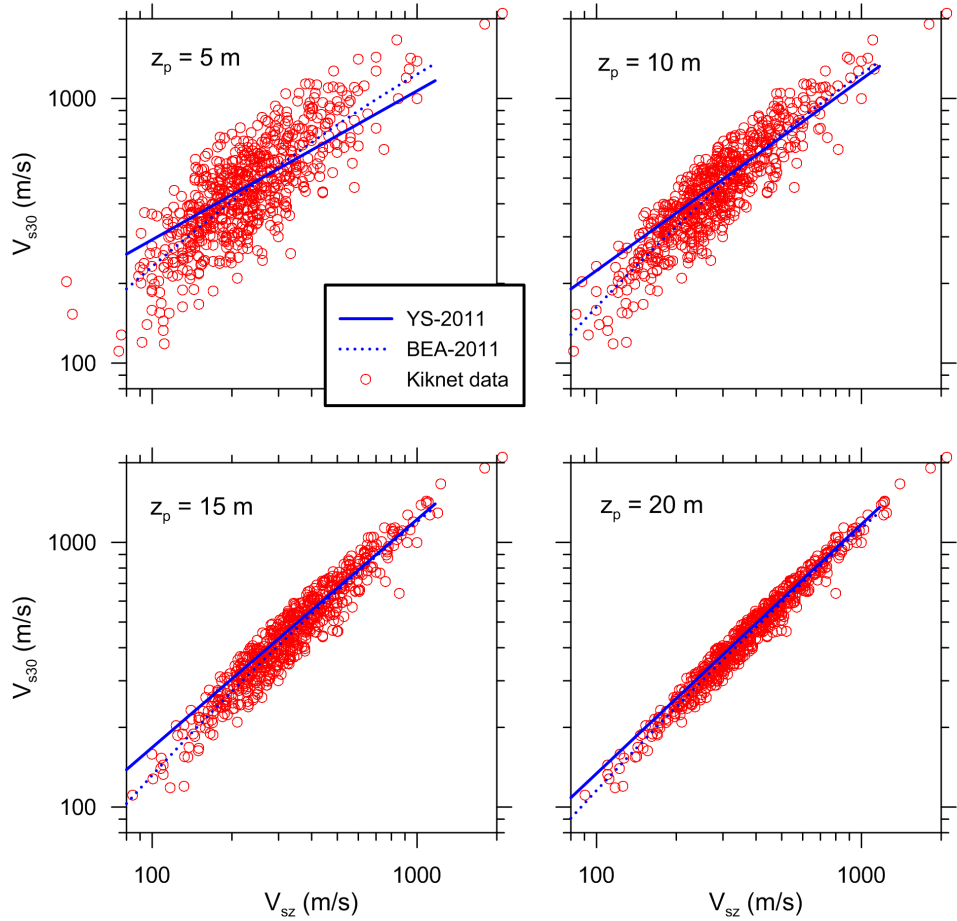


Figure 2.11 Comparison of Vs30-Vsz relationships developed by Yu and Silva and Boore *et al* [2011] with Kiknet data for four profile depths, z_p .

2.5 Discussion of Methods and Comparison

While it is clear that V_{s30} is most reliably obtained with high-quality geophysical measurements at the site of interest, no consensus exists regarding how it should be estimated in the absence of such measurements. In many cases, practical considerations may dictate the choice of method to be applied in a given area; for example, in the absence of geological maps, topography-based methods are the only viable option. However, when the available information does provide options (e.g., when both high quality geological and topographic information are available), which method should be selected? Ideally this decision would be made on the basis of local or regional studies of the efficacy of these techniques to the region. Given the currently available information, we investigate the relative reliability of the techniques described above through analysis of the dispersion of prediction residuals.

The dispersion for a given V_{s30} -estimation method is derived from statistical analysis of residuals:

$$R_V = \ln(V_{s30})_{\text{meas}} - \ln(V_{s30})_{\text{est}} \quad (2.4)$$

where $(V_{s30})_{\text{meas}}$ is a measured value and $(V_{s30})_{\text{est}}$ is estimated based on a correlation relationship. Note that by taking the natural log of the data, we assume the velocities to be log-normally distributed. The median of residuals should be zero in the absence of model bias. The standard deviation of residuals (denoted σ_{nv}) can be calculated for the entire set of residuals or sub-sets having certain conditions (e.g., subsets within certain site categories). Standard deviation term σ_{nv} represents epistemic uncertainty on velocity, which should be

considered in ground motion estimation. Boore *et al* [2011] describe procedures by which this uncertainty can be considered in ground motion evaluation from GMPEs.

For the case of geology-based correlations, statistical analyses by Moss [2008] of V_{s30} arithmetic residuals (i.e., not in log units) indicates coefficients of variation (COVs) as shown in Figure 2.12, which range from approximately 0.15 for soft soils to 0.55 for crystalline rock. The COV is comparable to the standard deviation of a log normal distribution [Ang and Tang, 1975, p 105] for small COV ($< \sim 0.3$).

For the Geomatrix-based correlations, we use the natural log standard deviations ($\sigma_{\ln V}$) from Table 2.6. For ground slope, we utilize the histogram shown in Figure 2.9, which indicates a standard deviation $\sigma_{\ln V} = 0.14 \times \ln(10) = 0.32$. Standard deviations separated into various ranges of ground slope are not presently available (David Wald, *personal communication*, [2011]). For terrain, we use $\sigma_{\ln V}$ from Table 2.4.

Figure 2.12 shows natural log standard deviation terms ($\sigma_{\ln V}$) for each of the V_{s30} estimation techniques described previously in this chapter, using the information sources described above. As noted previously, these $\sigma_{\ln V}$ measurements represent the epistemic uncertainty. Dispersion was separated by categories when practical as indicated in the figure and caption. For comparison, Figure 2.13 also shows standard deviations for V_{s30} based on measurements, taken from the COV results from Moss [2008], which are based principally on sites with multiple V_s measurements. Measurement-based COVs would be expected to be higher than those given by Moss when the site geology is highly heterogeneous and V_s measurements are widely spaced relative to the scale of the site variability. For example, the NGA site spreadsheet from the original NGA project (Darragh, *personal communication*, [2011]) allows a borehole to be associated with a ground motion station for separation distances up to 300 m, and assigns a dispersion to the value of V_{s30} ranging from 0.05 for soft soil to 0.3 for firm rock.

As expected, none of the estimation techniques (other than V_{sz} - V_{s30} relations) are able to reproduce the low dispersions from measurement. We generally see lower dispersion for softer sites, represented by Quaternary geology, Geomatrix categories C-E, and terrain categories 8, 12, and 16. The surface geology and GMX schemes are similar in their use of geologic context to establish categories. Comparing these two, the geology scheme tends to have slightly lower dispersion for comparable conditions (e.g., Qi/Qa versus D/E; M rock vs A). It is difficult to compare the topography-based methods (slope vs terrain) because we do not have the slope data separated according to the various V_{s30} categories as shown in Table 2.1. We note that the dispersion for the slope-based method is in the general range of the dispersions from the surface geology and GMX methods. The terrain-based method provides the lowest dispersions for categories associated with young sediments (12, 16), but also produces high dispersions for some rock categories (3, 7). The V_{sz} - V_{s30} relation produces lower dispersion than any of the other correlations for $z_p > 10$ m, and such methods are preferred when geophysical data are available.

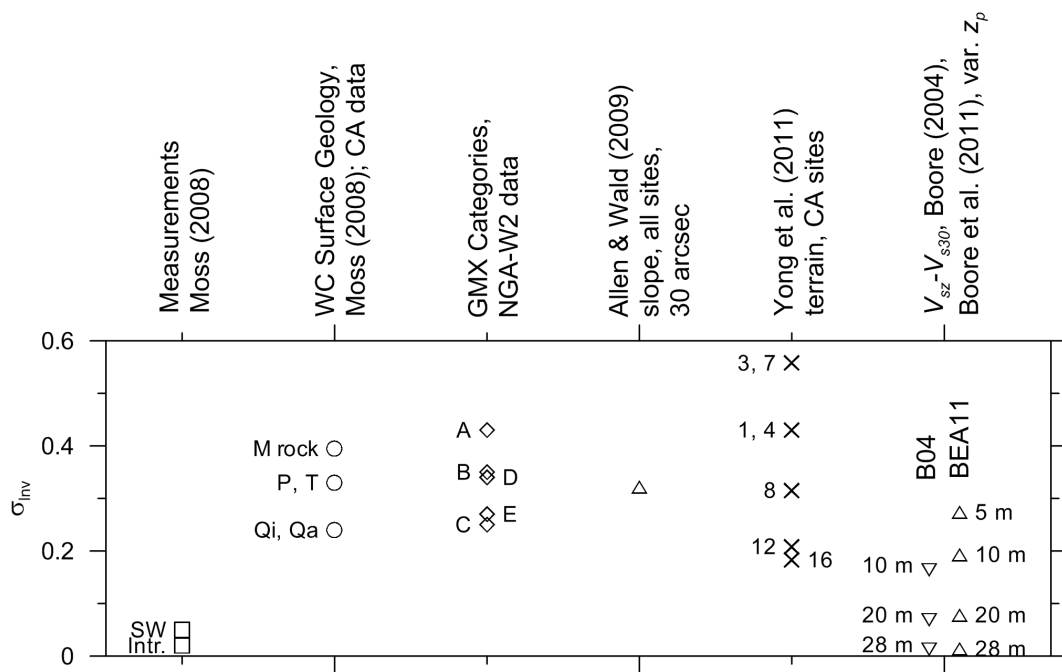


Figure 2.12: Dispersion of Vs30 prediction residuals reported as natural log standard deviation ($\sigma\ln V$). Results from Moss [2008] are COVs taken as approximately equal to $\sigma\ln V$. Explanation of codes. Measurements: SW = surface wave methods, Intr = intrusive methods (borehole). Surface geology: M rock = Mesozoic rock categories, P, T = Pleistocene and Tertiary categories, Qi, Qa = Quaternary mud and alluvium categories. GMX: A-E, see Table 2.2. Terrain: numbered categories, see Table 2.4.

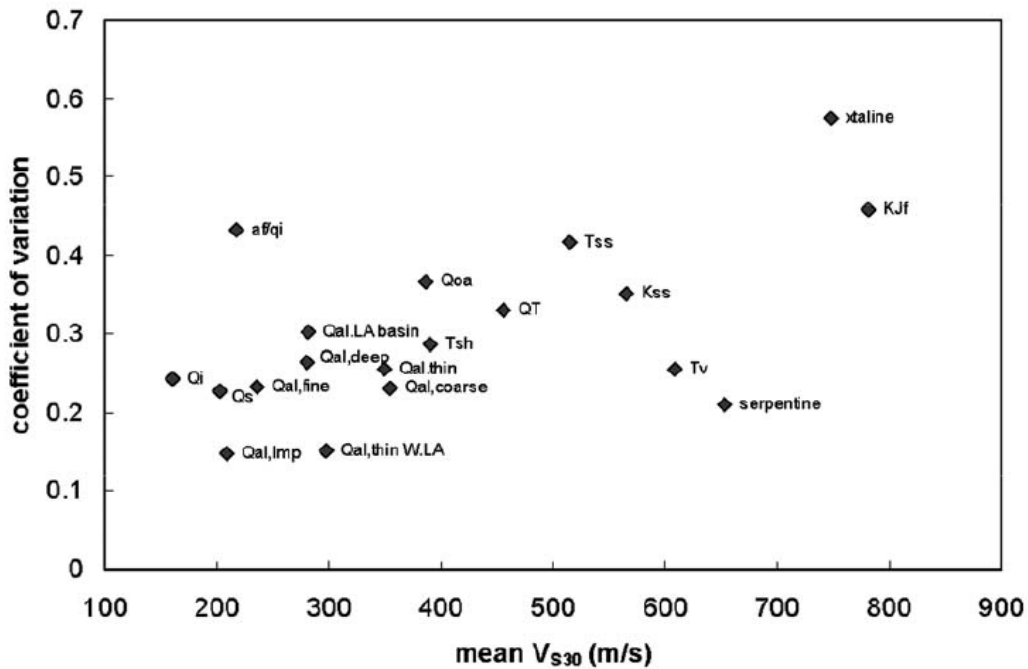


Figure 2.13 COV of Vs30 values estimated using geologic correlations by Wills and Clahan [2006]. From Moss [2008]

3 Estimation of Basin Depth

Basin depth is parameterized in three of the NGA GMPEs using Z_x , which is the depth to a shear wave isosurface having $V_s = x$ km/sec. Abrahamson and Silva [2008] and Chiou and Youngs [2008a] take $x=1.0$ km/sec while Campbell and Bozorgnia take $x = 2.5$ km/sec. As noted in Paragraph B.2, aside from the NGA models, other GMPEs have not utilized basin depth for site parameterization. Basin depth models for particular regions have been developed from various geophysical data sources including gravity surveys, reflection/refraction surveys, and deep boreholes.

The Southern California Earthquake Center (SCEC) has developed a depth model for southern California that includes the Ventura, San Fernando Valley, Los Angeles, San Bernardino, and Imperial Valley basins. Versions of SCEC basin model have been presented by Magistrale *et al* [2000] and Kohler *et al* [2003]; the most recent version is referred to as CVM-Version 4 [4]. This model has been used to develop basin depth terms Z1.0 and Z2.5 for ground motion recording stations, which are contained in the site database for the NGA-West 2 project [1].

The USGS has developed models for the seismic velocity structure in the San Francisco Bay Area (SFBA) region, which are presented in Boatwright *et al* [2004], Brocher [2005] and Hardebeck *et al* [2007]. As with the SCEC model, a recent version of this model (RW Graves, personal communication, [2011] was used to estimate Z1.0 and Z2.5 for recording sites in the study region, which are contained NGA-West 2 site database.

Additional basin models that have been used in ground motion simulations, but not necessarily to extract depth parameters for empirical ground motion studies, include:

- State-wide California models based on tomography [Lin *et al*, 2010]
- Eel River basin in northern California [Graves, 1994]
- Puget Sound and Seattle areas (e.g., Symons and Crosson, [1997]; Brocher *et al*, [2001])
- Tokyo Bay region, Japan [Sato *et al*, 1999]
- Osaka and Kobe regions, Japan [Kagawa *et al*, 2004]
- Adapazari basin, Turkey [Goto *et al*, 2005]

The practicality of open access to these basin models for GMPE applications is unknown. In many areas where the NGA GMPEs are applied, basin models are either unavailable or inaccessible. Options for dealing with the basin term in such cases include selecting a depth parameter that “turns off” the basin amplification factor (makes the term zero) or correlating basin depth to other available information. The “turn-off” feature can be implemented as follows:

- Abrahamson and Silva [2008]: Select Z1.0 as the average value for a given V_{s30} using equations provided by Abrahamson and Silva (see Equation 3.1 below).
- Campbell and Bozorgnia [2008]: Select Z2.5 between 1 and 3 km.

- Chiou and Youngs [2008a]: Select Z1.0 as a value smaller than their Φ_7 parameter, which is given in Table 3 of Chiou and Youngs and takes values between 300 and 600 m.

Using data from the NGA-West2 site database at sites with measurements of V_{s30} and values of basin depth extracted from the SCEC and USGS models, we plot in Figure 3.1 the relationship between V_{s30} and $Z_{1.0}$. The data follow a trend of increasing $Z_{1.0}$ with decreasing V_{s30} in both study regions. The following fit equations are also plotted through the data:

$$\begin{aligned} & 6.745 \quad V_{s30} < 180 \text{ m/s} \\ & \ln(\bar{Z}_{1.0}) = 6.745 - 1.35 \ln\left(\frac{V_{s30}}{180}\right) \quad 180 < V_{s30} < 500 \text{ m/s} \\ & 5.394 - 4.48 \ln\left(\frac{V_{s30}}{500}\right) \quad V_{s30} > 500 \text{ m/s} \end{aligned} \quad (3.1)$$

$$\ln(\bar{Z}_{1.0}) = 28.5 - \frac{3.82}{8} \ln(V_{s30}^8 + 378.7^8) \quad (3.2)$$

Equation 3.1 was developed by Abrahamson and Silva [2008] and Equation 3.2 was developed by Chiou and Youngs [2008a] using different versions of the SCEC 3D basin model, not actual data.

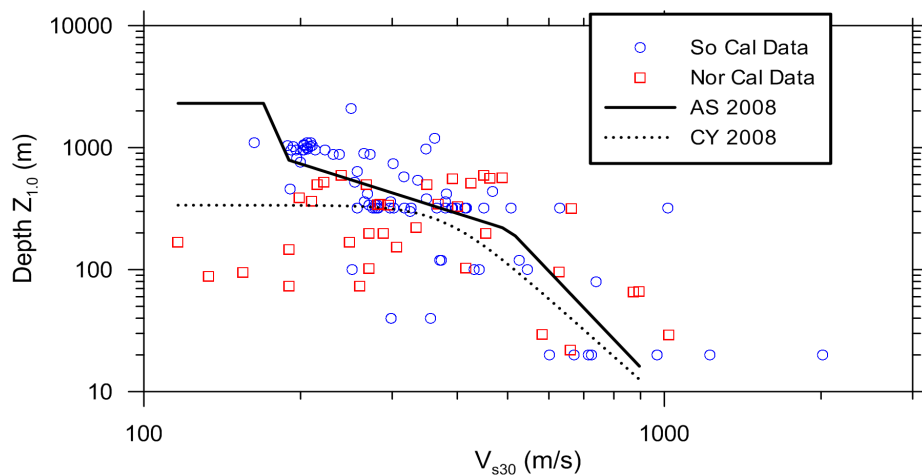


Figure 3.1 Trend of basin depth $Z_{1.0}$ with V_{s30} and fit models proposed by Abrahamson and Silva [2008] and Chiou and Youngs [2008a]. Data from NGA-West2 site database.

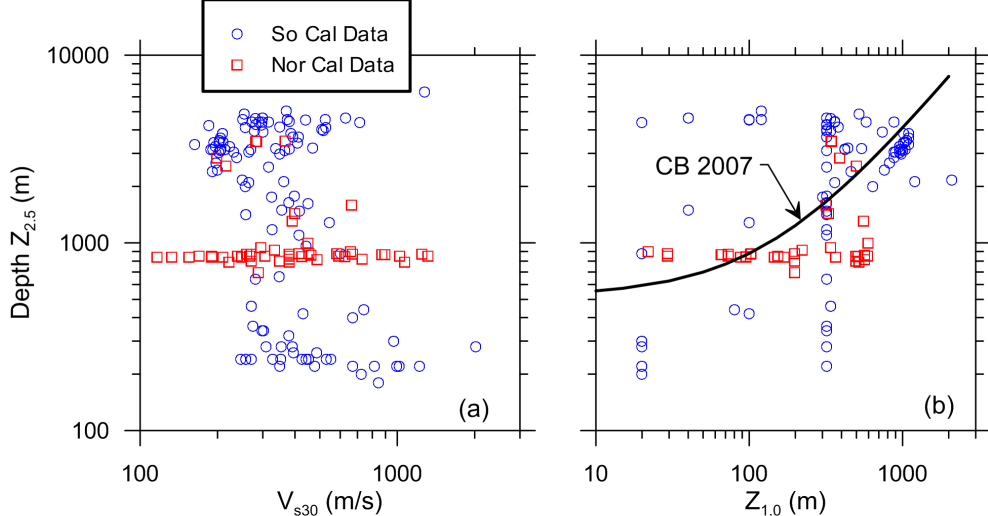


Figure 3.2 Trend of basin depth $Z_{2.5}$ with (a) V_{s30} and (b) depth $Z_{1.0}$ along with fit model proposed Campbell and Bozorgnia [2007].

As shown in Figure 3.1, the models are similar for $V_{s30} > 200$ m/sec and both fit the data reasonably well in that velocity range. At lower velocities, the AS model appears to more closely track the southern California data whereas the CY is closer to the SFBA data.

Figure 3.2a shows that $Z_{2.5}$ does not correlate with V_{s30} , and indeed no correlation relationships for these parameters were developed in the NGA project. Figure 3.2b shows the relationship between $Z_{2.5}$ and $Z_{1.0}$ along with the following correlation relationship between these parameters from Campbell and Bozorgnia [2007]:

$$\bar{Z}_{2.5} = 519 + 3.595Z_{1.0} \quad (3.3)$$

The $Z_{2.5}$ - $Z_{1.0}$ trend does not appear as strong as the $Z_{1.0}$ - V_{s30} trend.

The models given in Equations 3.1 through 3.3 for estimation of basin depth parameters are specific to the regions in California for which the basin models were developed. Their applicability to other geologic environments is unknown. In the absence of local studies in which the reliability of the models is verified, we do not recommend their use elsewhere. It would be preferred to “turn off” the basin terms in the manner described above for such situations.

4 Summary and Conclusions

The objectives of this report were to (1) review the site parameters used in GMPEs world-wide for various tectonic regimes and (2) describe procedures for estimation of site parameters in the absence of site-specific data.

As described in Chapter 1, most modern GMPEs use either V_{s30} directly as a continuous variable site parameter or as the basis for site classification into discrete categories. Three GMPEs developed for active regions in the NGA project also use basin depth parameters Z_x that represent depth to a shear wave isosurface with $V_s = x$ km/sec. Accordingly, we emphasized in this report estimation procedures for V_{s30} and Z_x , where $x=1$ or 2.5 km.

For site-specific applications, we recommend that V_{s30} be developed from on-site geophysical measurements. When those measurements extend to a depth $z_p < 30$ m, V_{s30} can be estimated using extrapolation methods described in Paragraph 2.4 with a higher degree of reliability than other estimation procedures.

In the absence of on-site geophysical data, or for regional ground motion studies, estimation of V_{s30} from geological or topographic data will generally be required. Geology- and terrain-based correlations are available [Wills and Clahan, 2006; Yong *et al*, 2011] that are calibrated against California data. Ground slope correlations are available that utilize additional data sources from specific regions world-wide. Some promising recent work utilizes ground slope correlations conditioned on a particular geologic unit [Wills and Gutierrez, 2008].

Previous work has shown that applying V_{s30} correlations for one region to another can be problematic, as demonstrated for example for bedrock condition in Italy by Scasserra *et al* [2009] and for Wenchuan, China sites generally by Yu and Silva (2011, personal communication with R. Darragh). Accordingly, we recommend local verification (and perhaps re-calibration) of V_{s30} estimation procedures when they are applied outside of the original study area. Additional discussion of work of this type will be presented in the forthcoming Task 6 report for the GEM Global GMPEs project.

When correlation relationships are used to estimate V_{s30} , there is a large epistemic uncertainty in the mean estimate, as represented by the σ_{Inv} term shown in Figure 2.12. This epistemic uncertainty should be considered in ground motion hazard analysis.

Basin depth parameter $Z_{1.0}$ has been shown to be reasonably well correlated to V_{s30} for California basins. Estimation procedures for $Z_{2.5}$ are weaker. These models have not been checked for geologic conditions outside of California and it is not recommended that they be applied for such conditions. Instead, we recommend the basin terms in the NGA GMPEs be “turned off” for such conditions using the guidelines given in Chapter 3.



References

- Abrahamson N.A., Silva W.J. [2008] "Summary of the Abrahamson and Silva NGA ground-motion relations," *Earthquake Spectra*, Vol. 24, pp. 67–97.
- Akkar S., Bommer J.J. [2010] "Empirical equations for the prediction of PGA, PGV and spectral accelerations in Europe, the Mediterranean region and the Middle East," *Seismological Research Letters*, Vol. 81, No. 2, pp. 195–206.
- Allen T., Wald D.J. [2009] "On the use of high-resolution topographic data as a proxy for seismic site conditions (VS30)," *Bulletin of the Seismological Society of America*, Vol. 99, No. 2A, pp. 935–943.
- Ang H.S., Tang W.H. [1975] *Probability Concepts in Engineering Planning and Design*, Vol. I, John Wiley and Sons, Inc., New York, Hyd. Div. Proc. ASCE
- Arroyo D., García D., Ordaz M., Mora M.A., Singh S.K. [2010] "Strong ground-motion relations for Mexican interplate earthquakes," *Journal of Seismology*, Vol. 14, No. 4, pp. 769–785.
- Atkinson G.M. [2008] "Ground-motion prediction equations for eastern North America from a referenced empirical approach: Implications for epistemic uncertainty," *Bulletin of the Seismological Society of America*, Vol. 98, No. 3, pp. 1304–1318.
- Atkinson G.M. [2010] "Ground-motion prediction equations for Hawaii from a referenced empirical approach," *Bulletin of the Seismological Society of America*, Vol. 100, No. 2, pp. 751–761.
- Atkinson G.M., Boore D.M. [2003] "Empirical ground-motion relations for subduction zone earthquakes and their application to Cascadia and other regions," *Bulletin of the Seismological Society of America*, Vol. 93, No. 4, pp. 1703–1729.
- Atkinson G.M., Boore D.M. [2006] "Earthquake ground-motion prediction equations for eastern North America," *Bulletin of the Seismological Society of America*, Vol. 96, No. 6, pp. 2181–2205.
- Atkinson G.M., Boore D.M. [2008] "Erratum: Empirical ground-motion relations for subduction zone earthquakes and their application to Cascadia and other regions," *Bulletin of the Seismological Society of America*, Vol. 98, No. 5, pp. 2567–2569.
- Atkinson G.M., Boore D.M. [2011] "Modifications to existing ground-motion prediction equations in light of new data," *Bulletin of the Seismological Society of America*, Vol. 101, No. 3, pp. 1121–1135.
- Atkinson G.M., Macias M. [2009] "Predicted ground motions for great interface earthquakes in the Cascadia subduction zone," *Bulletin of the Seismological Society of America*, Vol. 99, No. 3, pp. 1552–1578.

- Boatwright J., Blair L., Catchings R., Goldman M., Perosi F., Steedman C. [2004] "Using twelve years of USGS refraction lines to calibrate the Brocher and others (1997) 3D velocity model of the Bay Area," *USGS Open File Report 2004-1282*.
- Boore DM. [2004] "Estimating Vs30 (or NEHRP site classes) from shallow velocity models (depth < 30 m)," *Bulletin of the Seismological Society of America*, Vol. 94, pp. 591–597.
- Boore D.M., Atkinson G.M. [2008] "Ground-motion prediction equations for the average horizontal component of PGA, PGV, and 5%-damped PSA at spectral periods between 0:01 s and 10:0 s," *Earthquake Spectra*, Vol. 24, No. 1, pp. 99–138.
- Boore D.M., Thompson E.M., Cadet H. [2011] "Regional correlations of Vs30 and velocities averaged over depths less than and greater than 30 m," *Bulletin of the Seismological Society of America*, Vol. 101, No. 6, pp. 3046–3059.
- Bose M., Sokolov V., Wenzel F. [2009] "Shake map methodology for intermediate-depth Vrancea (Romania) earthquakes," *Earthquake Spectra*, Vol. 25, No. 3, pp. 497–514.
- Brocher T.M., Parsons T., Blakely R.J. et al [2001] "Upper crustal structure in Puget Lowland, Washington: Results from the 1998 Seismic Hazards Investigation in Puget Sound," *Journal of Geophysical Research-Solid Earth*, Vol. 106, No. B7, pp. 13541–13564.
- Brocher T.M. [2005] "Compressional and shear wave velocity versus depth in the San Francisco Bay Area, California: Rules for USGS Bay area velocity model 05.0.0," *USGS Open-File Report 2005-1317*, 58 pgs.
- Cadet H., Duval A.-M. [2009] "A shear wave velocity study based on the KiK-net borehole data: A short note," *Seismological Research Letters*, Vol. 80, pp. 440–445.
- Campbell K.W. [2003] "Prediction of strong ground motion using the hybrid empirical method and its use in the development of ground-motion (attenuation) relations in eastern North America," *Bulletin of the Seismological Society of America*, Vol. 93, No. 3, pp. 1012–1033.
- Campbell K.W., Bozorgnia Y. [2007] "Campbell-Bozorgnia NGA ground motion relations for the geometric mean horizontal component of peak and spectral ground motion parameters," *PEER Report No. 2007/02*, Pacific Earthquake Engineering Research Center, University of California, Berkeley, CA.
- Campbell K.W., Bozorgnia Y. [2008] "NGA ground motion model for the geometric mean horizontal component of PGA, PGV, PGD and 5% damped linear elastic response spectra for periods ranging from 0:01 to 10 s.," *Earthquake Spectra*, Vol. 24, No. 1, pp. 139–171.
- Cauzzi, C., Faccioli, E. [2008] "Broadband (0.05 to 20 s) prediction of displacement response spectra based on worldwide digital records," *Journal of Seismology*, Vol. 12, No. 4, pp. 453–475.
- CEN [2004] "Eurocode 8 - design of structures for earthquake resistance. Part 1: general rules, seismic actions and rules for buildings," European standard EN 1998-1, European Committee for Standardization, Brussels.
- Chiou B.S.J., Youngs R.R. [2008a] "An NGA model for the average horizontal component of peak ground motion and response spectra," *Earthquake Spectra*, Vol. 24, No. 1, pp. 173–215.

- Chiou B.S.J., Youngs R.R. [2008b] "Chiou and Youngs PEER-NGA empirical ground motion model for the average horizontal component of peak acceleration, peak velocity, and pseudo-spectral acceleration for spectral periods of 0.01 to 10 seconds," *Final Report*, Pacific Earthquake Engineering Research Center, University of California, Berkeley, CA.
- Di Alessandro C., Bonilla L.F., Boore D.M., Rovelli A., Scotti O. [2011] "Predominant-period site classification for response spectra prediction equations in Italy", *Bulletin of the Seismological Society of America*, Vol. 102, No. 2, 680–695.
- Douglas J., Bungum H., Scherbaum F. [2006] "Ground-motion prediction equations for southern Spain and southern Norway obtained using the composite model perspective," *Journal of Earthquake Engineering*, Vol. 10, No. 1, pp. 33–72.
- Faccioli E., Bianchini A., Villani M. [2010] "New ground motion prediction equations for $T > 1$ s and their influence on seismic hazard assessment," *Proceedings of Symposium on Long-Period Ground Motion and Urban Disaster Mitigation*, University of Tokyo, Japan.
- Farr T.G., Kobrick M. [2000] "Shuttle radar topography mission produces a wealth of data," *EOS Transactions*, Vol. 81, pp. 583–585.
- Franke, A., Mueller C., Barnhard T., Perkins D., Leyendecker E., Dickman N., Hanson S., Hopper M. [1996] "National seismic hazard maps: Documentation," *USGS Open-File Report 96-532*, 69 pgs.
- Fumal T.E., Tinsley J.C. [1985] "Mapping shear-wave velocities of near-surface geologic materials," in "Evaluating Earthquake Hazards in the Los Angeles Region-An Earth-Science Perspective.", (Ed. J.I. Ziony), *U.S. Geological Survey Professional Paper 1360*, pp. 101–126.
- Garcia D., Singh S.K., Herraiz M., Ordaz M., Pacheco J.F. [2005] "Inslab earthquakes of central Mexico: Peak ground-motion parameters and response spectra," *Bulletin of the Seismological Society of America*, Vol. 95, No. 6, pp. 2272–2282.
- Goto H., Sawada S., Morikawa H., Kiku H., Ozalaybey S. [2005] "Modeling of 3D subsurface structure and numerical simulation of strong ground motion in the Adapazari Basin during the 1999 Kocaeli earthquake, Turkey," *Bulletin of the Seismological Society of America*, Vol. 95, No. 6, pp. 2197–2215.
- Graves R.W. [1994] "Simulating the 3D Basin Response in the Portland and Puget Sound regions from large subduction zone earthquakes," *USGS Award 1434-93-G-2327*, Annual Technical Report.
- Hardebeck J. L., Michael, A. J., Brocher T. M. [2007] "Seismic velocity structure and seismotectonics of the eastern San Francisco Bay region, California," *Bulletin of the Seismological Society of America*, Vol. 97, pp. 826–842.
- Iwahashi J., Pike R.J. [2007] "Automated classifications of topography from DEMs by an unsupervised nested-means algorithm and a three-part geometric signature," *Geomorphology*, Vol. 86, No. 3-4, pp. 409–440.
- Iwahashi J., Kamiya I., Matsuoka M. [2010] "Regression analysis of Vs30 using topographic attributes from a 50-m DEM," *Geomorphology*, Vol. 117, No. 1-2, pp. 202–205.

- Kagawa T., Zhao B., Miyakoshi K., Irikura K. [2004] "Modeling of 3D basin structures for seismic wave simulations based on available information on the target area: case study of the Osaka Basin, Japan," *Bulletin of the Seismological Society of America*, Vol. 94, No. 4, pp. 1353–1368.
- Kanno T., Narita A., Morikawa N., Fujiwara H., Fukushima Y. [2006] "A new attenuation relation for strong ground motion in Japan based on recorded data," *Bulletin of the Seismological Society of America*, Vol. 96, No. 3, pp. 879–897.
- Kohler M.D., Magistrale H., Clayton R.W. [2003] "Mantle heterogeneities and the SCEC Reference Three-Dimensional Seismic Velocity Model Version 3," *Bulletin of the Seismological Society of America*, Vol. 93, pp. 757–774.
- Lin G., Thurber C.H., Zhang H., Hauksson E., Shearer P.M., Waldhauser F., Brocher T.M., Hardebeck J. [2010] "A California statewide three-dimensional seismic velocity model from both absolute and differential times," *Bulletin of the Seismological Society of America*, Vol. 100, No. 1, pp. 225–240.
- Lin P.-S., Lee C.T. [2008] "Ground-motion attenuation relationships for subduction-zone earthquakes in northeastern Taiwan," *Bulletin of the Seismological Society of America*, Vol. 98, No. 1, pp. 220–240.
- Magistrale H., Day S., Clayton R.W., Graves R.W. [2000] "The SCEC Southern California reference three-dimensional seismic velocity model version 2," *Bulletin of the Seismological Society of America*, Vol. 90, pp. S65–S76.
- McVerry G.H., Zhao J.X., Abrahamson N.A., Somerville P.G. [2006] "New Zealand acceleration response spectrum attenuation relations for crustal and subduction zone earthquakes," *Bulletin of the New Zealand Society of Earthquake Engineering*, Vol. 39, No. 4, pp. 1–58.
- Moss R.E.S. [2008] "Quantifying measurement uncertainty of thirty-meter shear-wave velocity," *Bulletin of the Seismological Society of America*, Vol. 98, No. 3, pp. 1399–1411.
- Okada Y., Kasahara K., Hori S., Obara K., Sekiguchi S., Fujiwara H., Yamamoto A. [2004] "Recent progress of seismic observation networks in Japan—Hi-net, F-net, K-NET and KiK-net," *Earth Planets Space*, Vol. 56, xv-xxviii.
- PEER GEM – Global GMPEs Task 2 WG: Douglas J., Cotton F., Abrahamson N.A., Akkar S., Boore D.M., Di Alessandro C. (2011) Pre-selection of ground-motion prediction equations (Task 2), Global GMPEs, Available from www.nexus.globalquakemodel.org/gem-gmpe/posts/.
- Pezeshk S., Zandieh A., Tavakoli B. [2011] "Hybrid empirical ground-motion prediction equations for eastern North America using NGA models and updated seismological parameters," *Bulletin of the Seismological Society of America*, Vol. 101, No. 4, pp. 1859–1870.
- Pilz M., Parolai S., Picozzi M., et al [2010] "Shear wave velocity model of the Santiago de Chile basin derived from ambient noise measurements: a comparison of proxies for seismic site conditions and amplification," *Geophysical Journal International*, Vol. 182, No. 1, 355–367.
- Raghu Kanth S.T.G., Iyengar R.N. [2006] "Seismic hazard estimation for Mumbai city," *Current Science*, Vol. 91, No. 11, pp. 1486–1494.

- Raghu Kanth S.T.G., Iyengar R.N. [2007] "Estimation of seismic spectral acceleration in peninsular India," *Journal Earth System Science*, Vol. 116, No. 3, pp. 199–214.
- Sato T., Graves R.W., Somerville P.G. [1999] 3-D finite-difference simulations of long-period strong motions in the Tokyo metropolitan area during the 1990 Odawara earthquake (MJ 5.1) and the great 1923 Kanto earthquake (MS 8.2) in Japan," *Bulletin of Earthquake Engineering*, Vol. 89, pp. 579–607.
- Scasserra G., Stewart J.P., Kayen R.E., Lanzo G. [2009] "Database for earthquake strong motion studies in Italy," *Journal of Earthquake Engineering*, Vol. 13, No. 6, pp. 852–881.
- Silva W.J., Gregor N., Darragh R. [2002] "Development of regional hard rock attenuation relations for central and eastern North America," *Report from Pacific Engineering and Analysis*, El Cerrito, California, 57 pgs.
- Sokolov V., Bonjer K.P., Wenzel F., Grecu G., Radulian M. [2008] "Ground-motion prediction equations for the intermediate depth Vrancea (Romania) earthquakes," *Bulletin of Earthquake Engineering*, Vol. 6, No. 3, pp. 367–388.
- Somerville P.G., Graves R.W., Collins N., Song S.G., Ni S., Cummins P. [2009] "Ground motion models for Australian earthquakes," *Report to Geoscience Australia*, URS Corporation.
- Symons, N.P., Crosson, R.S. [1997] "Seismic velocity structure of the Puget Sound region from 3-D non-linear tomography," *Geophysical Research Letters*, Vol. 24, No. 21, pp. 2593–2596.
- Thompson E.M., Baise L.G., Kayen R.E., Morgan E.C., Kakla manos J. [2011] "Multiscale site response mapping: A case study of Parkfield, California," *Bulletin of the Seismological Society of America*, Vol. 101, No. 3, pp. 1081–1100.
- Toro G.R., Abrahamson N.A., Schneider J.F. [1997] "Model of strong ground motions from earthquake in central and eastern North America: Best estimates and uncertainties," *Seismological Research Letters*, Vol. 68, No. 1, pp. 41–57.
- Wald D.J., Allen T.I. [2007] "Topographic slope as a proxy for seismic site conditions and amplification," *Bulletin of the Seismological Society of America*, Vol. 97, No. 5, pp. 1379–1395.
- Wills C.J., Clahan K.B. [2006] "Developing a map of geologically defined site-condition categories for California," *Bulletin of the Seismological Society of America*, Vol. 96, pp. 1483–1501.
- Wills C.J., Gutierrez C. [2008] "Investigation of geographic rules for improving site-conditions mapping," *Calif. Geological Survey Final Technical Report*, 20 pgs. (Award No. 07HQGR0061).
- Yong A., Hough S.E., Abrams M.J. et al [2008a] "Preliminary results for a semi-automated quantification of site effects using geomorphometry and ASTER satellite data for Mozambique, Pakistan and Turkey," *Journal Earth System Science*, Vol. 117, No. 2, pp. 797–808.
- Yong A., Hough S.E., Abrams M.J. [2008b] "Site characterization using integrated imaging analysis methods on satellite data of the Islamabad, Pakistan, Region," *Bulletin of the Seismological Society of America*, Vol. 98, No. 6, pp. 2679–2693.

Yong A., Hough S.E., Iwashashi J., Braverman A. [2011] "A terrain-based site characterization map of California with implications for the contiguous United States," *Bulletin of the Seismological Society of America*, Vol. 102, No. 1, pp. 114–128.

Youngs R.R., Chiou B.S.J., Silva W.J., Humphrey J.R. [1997] "Strong ground motion attenuation relationships for subduction zone earthquakes," *Seismological Research Letters*, Vol. 68, No. 1, pp. 58–73.

Zhao J.X. [2010] "Geometric spreading functions and modeling of volcanic zones for strong-motion attenuation models derived from records in Japan," *Bulletin of the Seismological Society of America*, Vol. 100, No. 2, pp. 712–732.

Zhao J.X., Zhang J., Asano A., Ohno Y., Oouchi T., Takahashi T., Ogawa H., Irikura K., Thio H.K., Somerville P.G., Fukushima Y. Fukushima, F. [2006] "Attenuation relations of strong ground motion in Japan using site classification based on predominant period," *Bulletin of the Seismological Society of America*, Vol. 96, No. 3, pp. 898–913.

Website references

1. Pacific Earthquake Engineering Research Center (PEER)

NGA-West 2 Project.

[Available at <http://peer.berkeley.edu/ngawest2/>]

2. United States Geological Survey

Earthquake Hazard Program

[Available at <http://earthquake.usgs.gov/hazards/apps/vs30/custom.php>]

3. Geospatial Information Authority of Japan (GSI)

Automated terrain classification map using SRTM 30

[Available at http://gisstar.gsi.go.jp/terrain/front_page.htm]

4. Southern California Earthquake Center (SCEC)

Three-Dimensional Community Velocity Model for Southern California (CVM-Version 4)

[Available at <http://www.data.scec.org/3Dvelocity>]